



## *In situ* visualization of Li concentration in all-solid-state lithium ion batteries using time-of-flight secondary ion mass spectrometry



Hideki Masuda<sup>a</sup>, Nobuyuki Ishida<sup>a,b,\*</sup>, Yoichiro Ogata<sup>c</sup>, Daigo Ito<sup>c</sup>, Daisuke Fujita<sup>a</sup>

<sup>a</sup> Research Center for Advanced Measurement and Characterization, National Institute for Materials Science, Japan

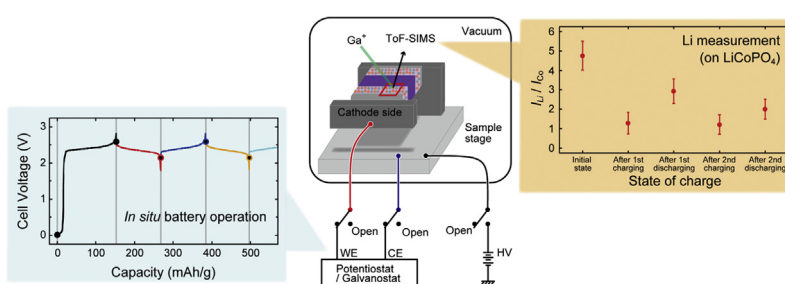
<sup>b</sup> Global Research Center for Environment and Energy Based on Nanomaterials Science (GREEN), National Institute for Materials Science, Japan

<sup>c</sup> R&D Center, TAIYO YUDEN CO., LTD., Japan

### HIGHLIGHTS

- We developed a novel ToF-SIMS combined with *in situ* electrical measurement.
- We visualized change in Li distribution at cathode composite of solid state LIB.
- Li in LiCoPO<sub>4</sub> exhibited cyclic increase and decrease following the operation.
- Li in solid electrolyte at cathode composite decreased after the first charging.

### GRAPHICAL ABSTRACT



### ARTICLE INFO

#### Keywords:

All-solid-state lithium ion batteries  
Time-of-flight secondary ion mass spectrometry  
Li ion mapping

### ABSTRACT

Lithium ion batteries (LIBs) are the most important energy storage devices. Novel methods for directly characterizing the behavior of Li ions during battery operations are highly coveted for understanding the fundamental working principles of the batteries and improving their device performances. In this study, we developed a novel method to visualize the change in Li ion distribution in the electrodes of all-solid-state (ASS) LIBs based on the time-of-flight secondary ion mass spectrometry technique with an *in situ* electrical measurement system. We succeeded in directly visualizing the decrease/increase of Li concentration in the cathode composite electrode during the charging/discharging cycles. Our method paves the way to characterize the fundamental aspects of ASS LIBs for improving device performance, including the evaluation of Li-depleted regions, visualization of the conductive paths and analysis of the causes of device degradation.

### 1. Introduction

Lithium ion batteries (LIBs) have become the most important energy storage devices owing to their high energy density and good cycle performance without memory effects. A strong demand exists for LIBs with enhanced performance for their application in portable devices and electric vehicles [1,2]. A detailed understanding of the complex electrochemical reactions occurring in the electrodes of LIBs is essential for improving LIB device performance as well as for device design

fabrication. One of the most important and uncomplicated methods for clarifying the working principle of LIBs is examining the behavior of Li ions during battery operations. However, it has been difficult to observe the distribution of Li ions in the electrodes owing to the lack of the measurement tools. The direct visualization of Li distribution changes during battery operation (*in situ* characterization) has been particularly challenging, and it has only been demonstrated once (in a very specific scenario) using scanning transmission electron microscopy [3]. In many cases, the behavior of Li ions in the electrodes has been estimated using

\* Corresponding author. Research Center for Advanced Measurement and Characterization, National Institute for Materials Science, Japan.

E-mail address: [ishida.nobuyuki@nims.go.jp](mailto:ishida.nobuyuki@nims.go.jp) (N. Ishida).

indirect methods, including measuring the change in geometry [4,5], lattice parameters [6,7], chemical-bonding states [8,9] and electrical potential of the electrode materials [10,11] during the Li insertion (desertion) into (out of) the electrodes.

Among the measurement tools available for the elemental mapping of sample surfaces, scanning electron microscopy-energy dispersive X-ray spectrometry (SEM-EDS) has been the most popular. However, the detection of Li ions using SEM-EDS is difficult because the X-ray emission probability from Li ions in Li compounds is very low [12]. On the other hand, scanning Auger microscopy can detect Li ions with high sensitivity [13–15]. However, the interpretation of data that is obtained from this technique is difficult due to electron beam-induced reduction of Li ions and the resultant segregation of Li metal [16]. In contrast to these two techniques, time-of-flight secondary-ion mass spectrometry (ToF-SIMS) can detect Li ions with high sensitivity and without electron beam-induced Li reduction. ToF-SIMS directly detects surface atoms by mass spectrometry of secondary ions sputtered using the primary ion beam. Therefore, any element can be detected in principle. In particular, Li can be detected with high sensitivity since it has high positive secondary ion efficiency. In fact, the mapping of Li distribution in the electrodes of LIBs using ToF-SIMS has been reported [17,18]. However, so far, the use of ToF-SIMS has been limited to disassembled electrode samples LIB devices after battery operation. Therefore, an *in situ* technique that can enable us to visualize the change of Li distributions in the electrodes during battery operations is highly coveted for investigating direct correlations between the behaviors of Li ions and battery performance.

In this work, we developed a novel method to directly observe the change of Li distribution in LIBs during normal battery operations using ToF-SIMS. This method is based on the following three key techniques: fabrication of a flat and clean cross-sectional surface using Ar-ion milling, fabrication of a home-made *in situ* electrical measurement system incorporated into the vacuum chamber of the ToF-SIMS and local sputtering of thin surface layers using the primary ion beam of the ToF-SIMS. With this method, we succeeded in directly visualizing the change in Li concentration during battery operation in the cathode composite electrode of an all-solid-state (ASS) LIB. Our technique can be applied to a wide range of ASS LIBs, including model LIBs as well as actual devices that have complex composite electrode structures. Thus, this technique can be an ideal method for characterizing various aspects of ASS LIBs for providing design criteria for the further improvement of LIB performance.

## 2. Experimental

### 2.1. Sample preparation

Fig. 1(a) shows the schematic of the ASS LIB used in this study. The ASS LIB used in this study comprised composite electrodes,  $\text{Li}_{1+x}\text{Al}_x\text{Ge}_{2-x}(\text{PO}_4)_3$  (LAGP) as a solid electrolyte and Pd as a current collector. For both the cathode and anode electrodes, we used the same composite structure, i.e., a mixture of  $\text{LiCoPO}_4$  (LCP),  $\text{Li}_{1+x}\text{Al}_x\text{Ti}_{2-x}(\text{PO}_4)_3$  (LATP) and Pd. In the cathode, LCP works as an active material, the LATP works as a solid electrolyte and Pd works as a conductive additive. The Pd conductive additive was used because Pd did not react with other materials nor disappeared during the co-sintering (at up to  $\sim 750^\circ\text{C}$ ) in the battery fabrication process, explained below. Also, Pd showed a good adhesive property with the solid electrolytes after the co-sintering process. The size of Pd particles after the co-sintering process ranged from 0.5 to  $2\ \mu\text{m}$ . In the anode, LATP works as the active material—a so-called “*in situ*-formed electrode system.” [19,20] The LCP and LATP (a NASICON-type solid electrolyte) are known to react with each other during the co-sintering process at high temperature [21,22]. To suppress this reaction, we used Co-doped LATP and LAGP [23]. The ASS LIB structure shown in Fig. 1(a) was fabricated by stacking the green ceramic sheets (on which each material is printed

using polyvinyl butyral as a binder) and subsequent co-sintering at up to  $\sim 750^\circ\text{C}$ . In the early stage of the co-sintering process at  $\sim 500^\circ\text{C}$ , the binders were completely removed. After the co-sintering, the relative density of the sample was  $\sim 95\%$ . This battery works at  $\sim 2.3\ \text{V}$  (LCP (4.8 V vs.  $\text{Li}/\text{Li}^+$ ) [24,25] to LATP (2.5 V vs.  $\text{Li}/\text{Li}^+$ ) [6,26]).

The LIB cells were stored in an Ar-filled glove box ( $\text{O}_2$ :  $< 0.8\ \text{ppm}$ ,  $\text{H}_2\text{O}$ :  $< 0.8\ \text{ppm}$ ) after the fabrication to avoid degradation. To prepare a sample for the ToF-SIMS measurements, a LIB cell was first cut into a  $1 \times 0.5\ \text{mm}^2$  piece in the Ar-filled glove box. Then, we transferred it into a vacuum chamber ( $\sim 10^{-4}\ \text{Pa}$ ) without exposure to air using the transfer vessel for polishing the cross-sectional surface with Ar-ion milling (JEOL IB-09020CP 8 kV). This process exposed the cross-sections of the particles of each material and flattened the entire cross-sectional surface. We confirmed that this process did not alter the LIB performance [11]. After the milling, the sample was again transferred into the Ar-filled glove box. In the glove box, we set the sample onto the sample holder for ToF-SIMS measurements. Subsequently, the sample holder was transferred into the introductory chamber of the ToF-SIMS ( $\sim 10^{-4}\ \text{Pa}$ ) using a home-made transfer vessel (Supplementary Fig. S1) without exposing the sample to air.

### 2.2. *In situ* ToF-SIMS measurement

We incorporated an *in situ* electrical measurement system into the ToF-SIMS system (Ulvac Phi, Phi Trift V) to perform battery operations without removing the samples from the vacuum chamber. Fig. 1(b and c) show a photograph and schematic illustration of the sample holder mounted on the sample stage of the ToF-SIMS. In this system, the sample is clamped by two stainless steel plates that are electrically isolated from each other. One of the two stainless steel plates is mechanically attached to the sample stage (made of stainless steel) of the ToF-SIMS. Each of the two stainless steel plates is electrically connected to a current-feedthrough attached to the vacuum chamber. Thus, by connecting an apparatus for electrical measurements to the feedthroughs outside the vacuum, we can operate the LIB while keeping the sample in the vacuum chamber. The electrical connection can be changed during ToF-SIMS measurements by toggling the mechanical switches so that one stainless steel plate of the sample holder (connected to the sample stage) is connected to the high voltage electrode and the other electrode is open.

Charging/discharging of the ASS LIBs was performed using a potentiostat-galvanostat (Princeton, VersaSTAT3-200) in the constant current mode. Fig. 1(d) shows charge/discharge characteristics of the LIB cell used in the ToF-SIMS measurement. The current density was 10 and  $5\ \mu\text{A}/\text{cm}^2$  for charging and discharging, respectively. The specific capacity was calculated for the cathode active material (LCP). The weight of the active materials (LCP) was calculated from the size of the sample and the volume ratio of LCP particles in the cathode composite (estimated from the ToF-SIMS elemental maps (Supplementary Fig. S2)). The cycling characteristics of the ASS LIB used for the ToF-SIMS measurements are shown in Supplementary Fig. S3.

We used the ToF-SIMS to evaluate the Li distribution in the cathode composite regions of the ASS LIB cross-sectional surface. The measurements were performed at the initial state and after each charge/discharge process during the battery operation cycle (marked by solid circles in Fig. 1(d)). During the ToF-SIMS measurements, the anode was connected to the sample stage (where a high voltage of 3 kV was applied) and the cathode was open (Fig. 1(c)). The vacuum pressure in the chamber was kept at  $\sim 10^{-7}\ \text{Pa}$ . We used a Ga ion beam accelerated at 30 kV in the un-bunched mode as the primary ion beam for high spatial resolution. The filament current was 1 nA and the beam size was  $\sim 50\ \text{nm}$ . A dose density of primary ion for each measurement was  $2.9 \times 10^{11}\ \text{ions}/\text{cm}^2$ . The ToF-SIMS spectra were measured at the points of  $256 \times 256$  pixels in the analysis area. Typical analysis area is  $15 \times 15\ \mu\text{m}^2$  or  $20 \times 20\ \mu\text{m}^2$ . A typical positive ion spectrum is displayed in Supplementary Fig. S2(a). We measured the mass spectrum

Download English Version:

<https://daneshyari.com/en/article/11005921>

Download Persian Version:

<https://daneshyari.com/article/11005921>

[Daneshyari.com](https://daneshyari.com)